result is obtained for $N_{large} = 220$ and $N_{small} = 200$ with 32.5% of the refined sets possessing mean phase errors less than 35°: 7.5, 10.0 and 15.0% in the ranges 0–25, 25–30 and 30–35°, respectively.

The TVAL structure was selected to show the capability of the tangent formula (12) to refine random phases in the case of a relatively large structure (156 nonhydrogen atoms in the unit cell). The best result was obtained for $N_{large} = 300$ and $N_{small} = 300$ ($\langle E_H \rangle = 1.24$). From a total of 200 sets, 12 (6%) show a mean phase error between 30 and 35°.

4. Concluding remarks

The viability of solving crystal structures from the direct interpretation of the nonorigin Patterson peaks as a function of the phases has been demonstrated. This result, however, should not be surprising since these peaks contain all the information regarding the atomic arrangement in the structure and, in addition, the atomicity information contained in the removed Patterson origin peak has already been considered in the derivation of the Fourier coefficients $G_H(\Phi)$.

This work was supported by the DGICYT (Project PB89-0036).

References

DEBAERDEMAEKER, T., TATE, C. & WOOLFSON, M. (1985). *Acta Cryst.* A**41**, 286–290.
KARLE, I. (1975). *J. Am. Chem. Soc.* **97**, 4379–4386.
KARLE, J. & HAUPTMAN, H. (1956). *Acta Cryst.* **9**, 635–651.
PATTERSON, A. (1935). *Z. Kristallogr. Teil A*, **90**, 517–542.
POYSER, J., EDWARDS, R., ANDERSON, J., HURSTHOUSE, M., WALKER, N., SHELDRICK, G. & WALLEY, A. (1986). *J. Antibiot.* **39**, 167–169.
RAMACHANDRAN, G. N. & RAMAN, S. (1959). *Acta Cryst.* **12**, 957–964.
ROSSMANN, M. & BLOW, D. (1962). *Acta Cryst.* **15**, 24–31.
SMITH, G., DUAX, W., LANGS, D., DETITTA, G., EDMONDS, J., ROHRER, D. & WEEKS, C. (1975). *J. Am. Chem. Soc.* **97**, 7242–7247.

Acta Cryst. (1993). A**49**, 409–421

Parametrization of Triply Periodic Minimal Surfaces. III. General Algorithm and Specific Examples for the Irregular Class

BY A. FOGDEN

Department of Applied Mathematics, Research School of Physical Sciences and Engineering, Australian National University, Box 4, Canberra 2601, Australia

(*Received* 11 *July* 1991; *accepted* 5 *October* 1992)

Abstract

The construction algorithm of the first two papers of this series [Fogden & Hyde (1992). *Acta Cryst.* A**48**, 442–451, 575–591] is extended to a general treatment of triply periodic minimal surfaces (containing as a special case the 'regular' class analysed previously). A detailed outline of the parametrization procedure for an arbitrary 'irregular' class surface is provided and verified *via* a systematic rederivation of the C(P) surface described by Neovius [*Bestimmung Zweier Speciellen Periodische Minimalflächen* (1883), Helsinki: Frenckel]. The method is further employed in parametrizing various empirically generated surfaces.

1. Introduction

Paper I of this series (Fogden & Hyde, 1992*a*) outlines the mathematical foundation of this study, in extending the local representation of a general minimal surface, due to Weierstrass, to a rigorous connection between infinite (triply) periodic minimal surfaces (IPMS) and the finite-sheeted Riemann surface of their algebraic complex Weierstrass functions. Topological considerations impose simple conditions relating the fundamental global characteristic of the IPMS – the genus – to the two principal global features of the Riemann surface – the total branch point order and number of sheets. Considerations of differential geometry local to the degenerate points of the IPMS (the 'flat' points, at which the Gaussian curvature is zero) constrain the Riemann surface structure to be local to the corresponding branch points. The local and global aspects are then coupled by the symmetries of the IPMS – the plane lines of curvature, linear asymptotes and rotational invariances – which reduce to Weierstrass functional relations. In summary, the specifying properties of an IPMS are readily translated into those of the Riemann surface, making the latter a natural and extremely useful means of describing the former.

The remainder of papers I and II of this series (Fogden & Hyde, 1992*a*,*b*) deals with a special subset

0108-7673/93/030409-13$06.00

of IPMS, the 'regular' class, for which each flat point has normal vector coincident only with those of other flat points possessing identical surface degeneracy. This corresponds to the simplest class of Riemann surfaces, permitting the above relationship to be harnessed in determining all possible 'regular' IPMS *via* enumeration of all possible Riemann surface structures. The resulting exhaustive listing of regular-class solutions is summarized in paper II. This list contains many of the low-genus/high-symmetry IPMS (such as the D, P and I-WP surfaces) postulated as modelling the underlying structures observed in a variety of molecular self-assemblies, *e.g.* aggregates in binary surfactant/water mixtures (Fontell, 1990). Recently, IPMS of more intricate topology, residing outside the 'regular' class, have been proposed as a description of phases exhibited in particular systems (Landh, 1992). In tandem with this development, a large number of new 'irregular' IPMS have been isolated, principally by the crystallographic methods of Fischer & Koch (1987, 1989) and Koch & Fischer (1988, 1989, 1990). Thus, the problem of parametrizing 'irregular' IPMS, dating back to Schwarz, is at present motivated by the experimentalists' need for precise mathematical definitions to accompany the expanding vocabulary of IPMS and hence permit the quantitative classification of observed structures. This problem is addressed in this study. Since much is borrowed from, and is a direct extension of, papers I and II, (Fogden & Hyde, 1992*a*,*b*) equations or tables of these papers will be indicated with I and II, respectively, to avoid unnecessary repetition.

2. Global and local constraints

Recall that the Gauss-map image of the fundamental unit of an IPMS is an s-fold covering of the unit sphere and hence of the complex ω plane on stereographic projection, representing the Riemann surface of the Weierstrass function $R(\omega)$. Thus the (algebraic) Weierstrass function is the solution $R=R(\omega)$ of an sth-degree polynomial equation (I3),

$$\sum_{M=0}^{s} a_M(\omega) R^M = 0, \tag{1}$$

for some set of polynomials $\{a_M(\omega)\}_{M=0}^{s}$. The requirements of topology and differential geometry in the large [outlined in (I6)–(I9)] relate the genus g of an orientable IPMS to the corresponding number of sheets s of the Riemann surface *via*

$$g = s+1 \tag{2}$$

and specify the total branch-point order W of the Riemann surface,

$$W = 4s. \tag{3}$$

Let $\{\omega_i\}_{i=1}^{n}$ denote the set of distinct flat-point normal-vector images of the IPMS fundamental unit. The number of surface points on the unit with common normal-vector image ω_i is equal to the generic value s if the multiplicity of the local Gauss-map degree is included. Equivalently, on the Riemann surface above ω_i, the Weierstrass-function value corresponding to a flat point of degree $b+1$ is represented by a branch point (of order b) pinning $b+1$ sheets there. In general, the points of the IPMS unit sharing this flat-point normal vector may possess differing Gauss-map degrees. Let the set $\{N_{ij}, b_{ij}\}_{j=0}^{n_i}$ represent the spectrum of branch points lying above ω_i on the s sheets of the Riemann surface. Here, $N_{ij}>0$ denotes the number of such branch points of order $b_{ij}>0$ for $j=1,\ldots,n_i$. By convention, $b_{i0}=0$, so $N_{i0}\geq 0$ is the number of sheets unbranched above ω_i. Hence, on summation,

$$\sum_{j=0}^{n_i} N_{ij}(b_{ij}+1) = s, \tag{4}$$

and the total branch-point order of the Riemann surface is

$$W = \sum_{i=1}^{n} W_i, \quad W_i = \sum_{j=1}^{n_i} N_{ij} b_{ij}, \tag{5}$$

so (3) implies

$$\sum_{i=1}^{n} W_i = \sum_{i=1}^{n} \sum_{j=1}^{n_i} N_{ij} b_{ij} = 4s. \tag{6}$$

In the special case of the regular class, $n_i=1$, $b_{i1}\equiv b_i$ and $N_{i0}=0$, which imply $N_{i1}=s/(b_i+1)$, so (6) recovers (I10) and, in particular, is no longer explicitly dependent upon s (*i.e.* upon the IPMS topology).

At a branch point of order b_{ij} above ω_i, (I2) implies that the corresponding Weierstrass-function value is infinite. Furthermore, local to ω_i, the divergent asymptotic forms of the $b_{ij}+1$ branches of the Weierstrass function pinned there are given by the $b_{ij}+1$ roots of the relation

$$R(\omega)^{b_{ij}+1} \sim r_{ij}(\omega-\omega_i)^{-a_{ij}}, \quad \omega\to\omega_i \tag{7}$$

for some complex constant r_{ij} and some positive integer a_{ij} coprime to $b_{ij}+1$. This a_{ij} is, in turn, related to b_{ij} *via* considerations of local differential geometry. Indeed, in Appendix A we prove that the two numbers coincide for any IPMS. Thus, from (7),

$$R(\omega) \sim \gamma_{ij}(\omega-\omega_i)^{-b_{ij}/(b_{ij}+1)}, \quad \omega\to\omega_i \tag{8}$$

[where γ_{ij} are the $b_{ij}+1$ roots of r_{ij}], a result established in paper I for the regular class only.

Hence our previous analysis provides the foundation for the present study, as a general IPMS recovers the regular-class Weierstrass functional form (together with its implications regarding local surface symmetries) in the vicinity of a branch point. In particular, the asymptotic methods in the Appendix of paper I may now be extended to the general case.

As before, the polynomials $a_M(\omega)$ in (1) are expressed for convenience as

$$a_M(\omega) = \alpha_M P_M(\omega) \prod_{i=1}^{n} (\omega - \omega_i)^{q_{Mi}}, \tag{9}$$

where $q_{Mi} \geq 0$, $P_M(\omega_i) \neq 0$ and α_s and α_0 are non-zero constants. The zeros of $R(\omega)$ are given by the zeros of the polynomial $a_0(\omega)$, so, since the requirement of pointwise-finite Gaussian curvature implies *via* (I2) that $R(\omega)$ is non-zero on $\mathbb{C}$, we have $a_0(\omega) \equiv \alpha_0$. Similarly, the points in $\mathbb{C}$ above which the Riemann surface is branched are precisely the zeros of the polynomial $a_s(\omega)$, hence $P_s(\omega) \equiv 1$. Furthermore, the order of the zero of $a_s(\omega)$ at ω_i is given by the branch-point order W_i of the Riemann surface over this point. Thus, from (5),

$$q_{si} = \sum_{j=1}^{n_i} N_{ij} b_{ij}. \tag{10}$$

Note that (6) then implies that the degree of the polynomial $a_s(\omega)$ is $4s$.

The case in which only the leading and zeroth terms $a_s(\omega)$ and $a_0(\omega)$ in (1) are present yields the regular class of IPMS analysed previously. For an 'irregular' IPMS, intermediate terms $a_{s-1}(\omega), \ldots, a_1(\omega)$ are present. Asymptotic constraints can then be utilized in determining the set $\{\deg P_M, \{q_{Mi}\}_{i=1}^{n}\}_{M=1}^{s-1}$ (where $\deg P_M$ denotes the degree of the polynomial P_M) characterizing the structure of the intermediate terms. These constraints, resulting from the requirement that the s roots $R(\omega)$ of the polynomial equation (1) recover the regular-class form in the special limits, yield a system of equalities and inequalities in the unknowns $\deg P_M$ and q_{Mi}. Some of the conditions may be satisfied trivially and provide no information. Others may lead to inconsistencies regarding a particular value of $\deg P_M$ or q_{Mi}, implying that the corresponding coefficient a_M must be set to zero and hence that the Mth term cannot be present in (1). The derivation of the constraints is detailed in Appendix *B*.

3. Symmetry constraints

The preceding asymptotic analysis yields no direct information regarding the complex numbers specifying the polynomials *via* (9), namely the constant coefficients $\{\alpha_M\}_{M=0}^{s}$, the branch-point positions $\{\omega_i\}_{i=1}^{n}$, and the zeros $\{\omega_{Mi}\}_{i=1}^{\deg P_M}$ of the polynomials $P_M (M = 1, \ldots, s-1)$,

$$P_M(\omega) = \prod_{i=1}^{\deg P_M} (\omega - \omega_{Mi}). \tag{11}$$

The qualitative nature of these parameters is obtained by addressing the symmetries of the IPMS, in particular, the plane lines of curvature, linear asymptotes and rotation and roto-inversion symmetries.

(*a*) *Plane lines of curvature and linear asymptotes*

A general analysis of plane lines of curvature and linear asymptotes on IPMS was presented in § 5 of paper I. It was shown that the conditions for the existence of these special curves (representing mirror planes and twofold axes, respectively) reduce to Weierstrass functional equations. The constraints on the unknown parameters in order that the defining equation (1) satisfies these relations are straightforward generalizations of the corresponding regular-class results and are summarized here.

For the representation (I1), the condition (I16) for a segment of the real axis $\mathrm{Im}\ \omega = 0$ to be the image of a line of curvature in the xz plane or an asymptote along the y axis is equivalent to (I17) and hence, on substitution of (1), to the identical condition

$$a_M(\bar{\omega}) = (\pm 1)^M \overline{a_M}(\omega) \tag{12}$$

for each coefficient polynomial (where the plus and minus signs refer to plane lines of curvature and linear asymptotes, respectively). This, in turn, implies from (9) and (11) that the sets of polynomial zeros are conjugate invariant

$$\{\overline{\omega_i}\} = \{\omega_i\}, \quad q_{Mi} \text{ constant}$$

and

$$\{\overline{\omega_{Mi}}\}_{i=1}^{\deg P_M} = \{\omega_{Mi}\}_{i=1}^{\deg P_M}, \tag{13}$$

and that the constants α_M satisfy

$$\alpha_M = (\pm 1)^M \overline{\alpha_M} \tag{14}$$

(and are hence either real or imaginary).

In general, the surface possesses a line of curvature in a plane with normal $\hat{\mathbf{n}} = (n_1, n_2, n_3)$ or an asymptote directed along its normal line if it satisfies the symmetry conditions, given by (I19), (I20) and (I22), with respect to the segment of the corresponding circle image $|n_3\omega + (n_1 + in_2)| = 1$ (for $n_3 \neq 0$) in the complex plane. The form (1) is consistent with the associated functional equation (I23) if the coefficient polynomials have the property

$$\begin{aligned} a_M(\bar{\omega}) = (\pm 1)^M & [n_3\bar{\omega} + (n_1 + in_2)]^{4M} \\ & \times \overline{a_M}([-(n_1 + in_2)\omega + n_3] \\ & \times [n_3\omega + (n_1 - in_2)]^{-1}). \end{aligned} \tag{15}$$

This demands that the sets of polynomial zeros are invariant on reflection in the image circle or, equivalently,

$$\{[-(n_1 + in_2)\bar{\omega}_i + n_3]/[n_3\bar{\omega}_i + (n_1 - in_2)]\} = \{\omega_i\}, \quad q_{Mi} \text{ constant}$$

and

$$\{[-(n_1 + in_2)\overline{\omega_{Mi}} + n_3]/[n_3\overline{\omega_{Mi}} + (n_1 - in_2)]\}_{i=1}^{\deg P_M} = \{\omega_{Mi}\}_{i=1}^{\deg P_M} \tag{16}$$

and that the number of such zeros [the degree of $a_M(\omega)$] is $4M$, that is,

$$\deg P_M + \sum_{i=1}^{n} q_{Mi} = 4M. \tag{17}$$

Furthermore, the arguments of the complex constants α_M are specified by the additional constraint

$$\alpha_M = (\pm 1)^M \prod_{i=1}^{n} [n_3\omega_i + (n_1 + in_2)]^{q_{Mi}} \times \prod_{i=1}^{\deg P_M} [n_3\omega_{Mi} + (n_1 + in_2)]\bar{\alpha}_M. \tag{18}$$

For the case of a branch point at infinity, say $\omega_n = \infty$, the condition (16) still applies to the set of $n-2$ finite branch points, say $\omega_2, \ldots, \omega_{n-1}$, permuted on reflection. It further applies to all n branch points if, with $\omega_1 = -(1/n_3)(n_1 + in_2)$ denoting the circle centre (imaged at infinity on reflection), we define $q_{Mn} = q_{M1}$. With this definition, (17) is unchanged and now implies that the degree of $a_M(\omega)$ is $4M - q_{M1}$ (or $4M$ if counted with the suppressed zero of order q_{M1} at infinity). In condition (18), the range of the first product is now restricted to the finite non-zero terms represented by $i = 2, \ldots, n-1$.

In the special case $n_3 = 0$, the generic image circle is now a ray through the origin at angle φ from the real axis such that $\exp(i\varphi) = n_2 + in_1$. With $n_3 = 0$ in (15), the corresponding rotated plane intersects the surface in a line of curvature or possesses a normal line coincident with a surface asymptote only if the ray defines a reflection axis of the polynomial zero sets

$$\{\overline{\exp(i\varphi)\omega_i}\} = \{\exp(i\varphi)\omega_i\}, \quad q_{Mi} \text{ constant}$$

and

$$\{\overline{\exp(i\varphi)\omega_{Mi}}\}_{i=1}^{\deg P_M} = \{\exp(i\varphi)\omega_{Mi}\}_{i=1}^{\deg P_M} \tag{19}$$

(where the point $\omega_n = \infty$ is invariant on ray reflection) and the constant-coefficient arguments satisfy the relation

$$\alpha_M = (\pm 1)^M \exp[i2\varphi(\deg P_M + \sum_{i=1}^{n-1} q_{Mi} - 2M)]\bar{\alpha}_M. \tag{20}$$

(*b*) *Rotation and roto-inversion symmetries*

The Weierstrass functional equations necessary for the IPMS to exhibit a rotational symmetry angle of φ' about the z axis (or roto-inversional symmetry on composition with inversion in the origin) were summarized in § 1(*b*) of paper II. For brevity, we restrict attention here to the on-surface symmetries. The surface is invariant on rotation (positive sign) or roto-inversion (negative sign) about the normal vector (projected to infinity in the complex plane) of a point (situated at the origin) provided

$$\exp(-i2\varphi')R(\exp(-i\varphi')\omega) = \pm R(\omega). \tag{21}$$

After substitution of this condition into (1), the corresponding condition in the polynomials $a_M(\omega)$ then implies that the zero sets are invariant under this rotation,

$$\{\exp(i\varphi')\omega_i\} = \{\omega_i\}, \quad q_{Mi} \text{ constant}$$

and

$$\{\exp(i\varphi')\omega_{Mi}\}_{i=1}^{\deg P_M} = \{\omega_{Mi}\}_{i=1}^{\deg P_M} \tag{22}$$

(with the point $\omega_n = \infty$ again fixed), and that, for each $M = 0, \ldots, s$,

$$(\pm 1)^M \exp\left[i\varphi'\left(\deg P_M + \sum_{i=1}^{n-1} q_{Mi} - 2M\right)\right] = 1 \quad (\text{or } \alpha_M = 0). \tag{23}$$

The set of equations (12)–(23) consider IPMS symmetry with respect to the complex plane representing the superposition of all s sheets of the Riemann surface. They relate the existence of surface symmetries to properties of the coefficient polynomials in the defining equation (1). In particular, each polynomial zero set $\{\omega_i\}_{i=1}^{n}$, $\{\omega_{Mi}\}_{i=1}^{\deg P_M}$ (counted with their multiplicities) must exhibit the associated symmetry in the complex plane. Furthermore, the nature of each constant coefficient α_M is determined (*i.e.* those which are zero are isolated and the argument of the non-zero values is specified). Hence, the analysis yields necessary conditions for the IPMS symmetry to be manifested on a particular number of sheets of the Riemann surface lying above the image in the complex plane. However, as opposed to the situation for the regular class, (1) cannot in general be inverted to obtain explicit expressions for the s branches of the Weierstrass function $R = R(\omega)$. Thus, from the above it is not possible to infer directly the global symmetry structure of the general Riemann surface, such as that performed in paper II.

4. Spherical geodesic tessellating polygons

From the discussion in paper I, the *Flächenstück* (or surface element) of an IPMS has as Gauss-map image a spherical geodesic polygon on the Riemann surface, the edges of which are the images of plane lines of curvature and/or linear asymptotes for the $\theta = 0$ (or $\theta = \pi/2$) member of the Bonnet associate family. Repeated reflection and/or rotation of the *Flächenstück* over these bounding curves generates the fundamental unit of the IPMS and, accordingly, reflection of the polygon in the corresponding edges results in

a tessellation of the s-sheeted Riemann surface over the sphere. On the projected spherical polygon unit there must therefore exist zeros (counted with their multiplicities) of each $a_M(\omega)$ such that, under this group of reflection operations, the polynomials defined by the complete set of zeros satisfy the constraints derived above.

Any such tessellating spherical geodesic polygon may be constructed from an underlying Schwarz triangular tiling, of a particular number of copies of the unit sphere, as a finite union of the triangles. The regular-class restriction that only branch points of the same order are superposed on the Riemann surface having been dispensed with, the underlying basis is now extended to all 15 Schwarz cases (Erdélyi, Magnus, Oberhettinger & Tricomi, 1953) and the constraint that the branch-point distributions must be identical on each underlying Schwarz tile of the Riemann surface is now relaxed. Hence, the zeros of each $a_M(\omega)$ allocated to the polygon unit can only be propagated to the entire Riemann surface by reflection across the underlying tile edges defining the polygon boundary: in general, no symmetry operations exist internal to the polygon relating the distribution on each constituent tile. However, with respect to superposition of the s-sheeted Riemann surface onto the complex plane, the complete distribution of zeros is necessarily symmetric on reflection across all underlying tile edges. Thus, each coefficient polynomial $a_M(\omega)$ may be expressed as some product of symmetric polynomial forms specific only to the particular Schwarz tiling employed.

In this way, the symmetry conditions derived above regarding the zero sets $\{\omega_i\}_{i=1}^{n}$, $\{\omega_{Mi}\}_{i=1}^{\deg P_M}$ of each $a_M(\omega)$ are an obvious requirement for consistency with the underlying tiling. The determination of the $a_M(\omega)$ then reduces to the appropriate choice of the symmetric polynomial forms comprising them. Furthermore, a given Schwarz tiling admits of a limited number of basic such forms only, classified by their degrees, thus facilitating enumeration of the finite set of possibilities meeting the constraints on the unknowns deg P_M and $\{q_{Mi}\}_{i=1}^{n}$ formulated earlier. A general discussion of the symmetric polynomial forms associated with a Schwarz tiling is presented in Appendix C.

The introduction of the underlying Schwarz tiling similarly permits the enumeration of all IPMS. In paper I, this was achieved for the regular class by expressing the global Riemann-surface constraint (3) as an equation [(I37)] relating the orders of the branch points assigned to the vertices $\{\lambda_j\pi\}_{j=1}^{3}$, edges and face of a single triangle. To generalize this, suppose that the polygon unit is the union of t triangles and let $\{b_{pj}\}_{j=1}^{3}$, $\{b'_{pk}\}_{k=1}^{N'}$ and $\{b''_{pl}\}_{l=1}^{N''}$ denote the orders of the branch points residing at the three vertices and on the edges and face, respectively, of the pth constituent triangle. Then, application of the Gauss–Bonnet theorem to the tessellation implies

$$\sum_{j=1}^{3}\lambda_j\left[(1/t)\sum_{p=1}^{t}b_{pj}/(b_{pj}+1)\right] + \sum_{k=1}^{N'}\left[(1/t)\sum_{p=1}^{t}b'_{pk}/(b'_{pk}+1)\right] + 2\sum_{l=1}^{N''}\left[(1/t)\sum_{p=1}^{t}b''_{pl}/(b''_{pl}+1)\right] = \Lambda, \quad (24)$$

where Λ is defined in (I35) and the regular-class result (I37) is the special case $t=1$.

A systematic derivation of all IPMS generated by a particular Schwarz tessellation demands solution of (24) for the set of possible orders of the branch-point distribution on the polygon unit. For the irregular class of IPMS, this equation depends explicitly on the number of underlying tiles t comprising the polygon [or, equivalently, (6) possesses an explicit s dependence]. Hence, (24) generates an infinity of IPMS candidates as t (and hence s) is increased without bound. For surfaces with a particular genus, this equation, in conjunction with supplementary necessary conditions, is an extremely useful tool for listing the finite set of possibilities.

5. Discriminant of the polynomial equation

To recapitulate the parametrization procedure to this stage, assume that, for a given IPMS, the *Flächenstück* is isolated and the nature of its Gauss-map image is established with respect to the corresponding underlying Schwarz tiling. From this, the basic structure of the entire Riemann surface tessellated by it is readily inferred. In particular, the nature of the flat-point images $\{\omega_i\}_{i=1}^{n}$ and the associated sets $\{N_{ij}, b_{ij}\}_{j=0}^{n_i}$ are known. The preceding analysis then determines the types of symmetric form defining each coefficient polynomial $a_M(\omega)$ in (1). The polynomials are then specified up to a number of real parameters: any degrees of freedom present in the symmetric forms (*i.e.* the γ_j in Appendix C), together with the constant coefficients α_M in (9) (effectively real quantities since their complex arguments are fixed by the symmetry conditions in § 3). The calculation of these final unknowns employs the remaining special feature of the Weierstrass function – its discriminant.

The most important characteristic of an algebraic function, defined by some polynomial equation (1), is the set of points ω that yield less than the generic number s of distinct function values $R(\omega)$. This includes the zeros of the leading coefficient polynomial $a_s(\omega)$, above which sheets of the Riemann surface are pinned at branch points. These are the flat-point images of the IPMS with Weierstrass function $R(\omega)$ and have been analysed above. The second type of special point, above which the function values coincide on some numbers of sheets of the Riemann

surface that are not pinned together there, are the zeros of the discriminant of the polynomial equation (1). With respect to an IPMS, this implies that, for a surface-normal vector corresponding in projection to a discriminant-zero ω, the set of s points on a fundamental unit possessing this common normal vector contains some number of distinct points with identical Weierstrass-function value $R(\omega)$. Now, from the Weierstrass representation (I1), two surface points with identical value of ω and $R(\omega)$ are locally indistinguishable in the context of the IPMS so they represent a degeneracy of the representation (which is only uniquely defined up to a rigid translation).

Surface normals corresponding to these discriminant zeros may be isolated *via* the symmetries of the Gauss-map image. Specifically, discriminant zeros occur at points of the underlying Schwarz tiling at which the angle subtended by the basic polygon unit (*Flächenstück* image) exceeds that of the Schwarz triangle. Furthermore, the particular nature of the degeneracy there is simply related to the ratio of these two angles. If it is required that the polynomial equation (1) evaluated at these points displays this degeneracy then this supplies additional equations necessary in determining the excess parameters remaining in the parametrization.

6. Parametrization of specific 'irregular' IPMS

To illustrate the parametrization method, IPMS with a variety of genera (and hence number of sheets in the Riemann surface) are considered. The symmetries of these IPMS relate to the underlying tilings given by Schwarz cases 1 and 4, for which the symmetric polynomial forms are detailed in Appendix *C*. The ensuing examples also require the formula for the discriminant D of a quadratic, cubic and quartic polynomial equation. For the equation

$$\sum_{m=0}^{d} \varphi_{d-m} z^m = 0,$$

the general discriminant formula gives

$$\begin{aligned}
d=2:\quad & D=-\varphi_0(\varphi_1^2-4\varphi_0\varphi_2);\\
d=3:\quad & D=\varphi_0(4\varphi_0\varphi_2^3-\varphi_1^2\varphi_2^2+4\varphi_1^3\varphi_3+27\varphi_0^2\varphi_3^2\\
& \quad -18\varphi_0\varphi_1\varphi_2\varphi_3);\\
d=4:\quad & D=(-1/27)\varphi_0[(27\varphi_1^2\varphi_4+27\varphi_0\varphi_3^2-9\varphi_1\varphi_2\varphi_3\\
& \quad -72\varphi_0\varphi_2\varphi_4+2\varphi_2^3)^2\\
& \quad +4(3\varphi_1\varphi_3-12\varphi_0\varphi_4-\varphi_2^2)^3]. \qquad (25)
\end{aligned}$$

The prefactor φ_0 in these formulae represents the trivial discriminant zeros due to the pinning of sheets at the branch points (the zeros of φ_0). The bracketed term then yields non-trivial discriminant zeros, at which the function value coincides on sheets that are not connected there.

(a) *The C(P) surface*

To illustrate the application of the construction algorithm, we use it to rederive the Weierstrass function of the C(P) surface, obtained by Neovius (1883) *via* a different and less generalizable analytic approach. For this IPMS, illustrated in Figs. 3(*a*) and 4(*a*)-(*c*) of the technical report by Schoen (1970), the Gauss-map image of the *Flächenstück* is given here in Fig. 1 with respect to the underlying Schwarz case 4 tiling. Here, the numbers indicate the orders of the flat-point images of the *Flächenstück* and the edges labelled p and l denote the images of the bounding plane-line-of-curvature and linear-asymptote segments.

It can be checked that this polygon unit, comprising four underlying triangles, satisfies the necessary condition (24). The set of orders of the branch points, residing here only at vertices [where $(\lambda_1, \lambda_2, \lambda_3)\pi = (\frac{1}{4}, \frac{1}{3}, \frac{1}{2})\pi$], is $\{\{b_{pj}\}_{p=1}^{4}\}_{j=1}^{3} = \{\{2,2,2,0\}, \{1,0,0,0\}, \{0,0,0,0\}\}$, which on substitution into the equation renders both sides equal to $\frac{1}{6}$, as required. The minimum number of these polygons required to tessellate a (multiple) covering of the unit sphere is the number of distinct polygon positions with respect to the underlying tiling. Now there are six $\pi/4$ vertices of the tiling, each of which offers eight distinct positions for the single $\pi/4$ vertex of the polygon, giving in total 48 distinct configurations. As this is the case for all three vertex types, there are 48 distinct polygon positions and the unit thus tessellates four sheets.

The genus g of the C(P) surface is 9, hence (2) implies that the Riemann surface of the Weierstrass function possesses $s = 8$ sheets, comprising two identical copies of the four-sheeted polygon tessellation.

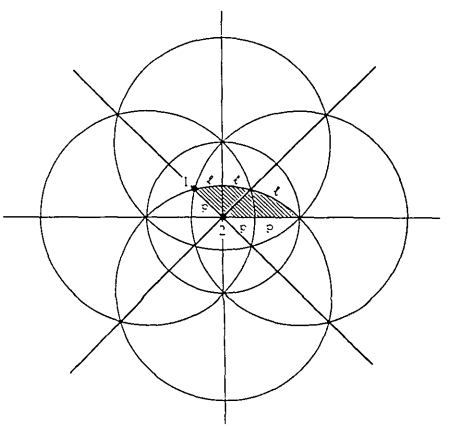

Fig. 1. Stereographic projection of the Schwarz case 4 tiling of the unit sphere, bearing the Gauss-map image (shaded region) of the C(P) surface *Flächenstück*. The *Flächenstück* is delimited by a pair of plane lines of curvature and a linear asymptote, with the edges marked with symbols '*p*' and '*l*', respectively. The small filled circles • denote the sites of flat points on the image; the assigned numerals give their order (a convention used throughout Figs. 1-5).

The two identical copies are indicative of the on-surface centres of inversion at the flat points corresponding to the first-order branch points, as the necessary requirement that $\varphi' = 0$ satisfies the negative root of (21) implies, *via* (23), that $\alpha_M = 0$ if M is odd. Hence, with only the even-power terms $M = 0, 2, 4, 6, 8$ present, the polynomial equation (1) becomes a quartic in R^2, where the four $\pm R$ branch pairs of the Weierstrass function correspond to the four pairs of identically tessellated sheets.

Now consider the Riemann-surface structure above the branched points of the Riemann surface, given by the polygon tessellation. On the eight sheets over each $\pi/4$ vertex of the underlying tiling, there exist three sheets pinned at a second-order branch point (exhausting the eight possible polygon positions with the $3\pi/4$ vertex at this site), together with three identically tessellated sheets pinned at a second such branch point (corresponding to the negated branches of the former) and an identically tessellated unbranched pair (each of which exhausts the eight positions with the $\pi/4$ vertex of the polygon situated there). Over each $\pi/3$ vertex of the tiling an identical pair is pinned at a first-order branch point (each spanned by the six configurations with the $\pi/3$ vertex of the polygon there) together with three identical unbranched pairs (representing the three possible orientations of the polygon edge at this underlying tiling vertex).

If the eight $\pi/3$ vertices and the six $\pi/4$ vertices of the underlying tiling (given in Appendix C) are denoted by $\{\omega_i\}_{i=1}^{8}$ and $\{\omega_i\}_{i=9}^{14}$, respectively (where $\omega_{14} = \infty$), the complete set of flat-point normal-vector images is $\{\omega_i\}_{i=1}^{14} = \{\omega_i\}_{i=1}^{8} U \{\omega_i\}_{i=9}^{14}$. Then the set $\{N_{ij}, b_{ij}\}_{j=0}^{1}$ of number N_{ij} of branch points of each order $b_{ij} \geq 0$ on the eight-sheeted Riemann surface above ω_i is $\{\{6, 0\}, \{1, 1\}\}$ for all $i = 1, \ldots, 8$ and $\{\{2, 0\}, \{2, 2\}\}$ for $i = 9, \ldots, 14$. We first determine the unknown parameters $\deg P_M$ and $\{q_{Mi}\}_{i=1}^{13}$ (for M even) for which, by virtue of the underlying tiling symmetry, q_{Mi} is identical for each $i = 1, \ldots, 8$ and each $i = 9, \ldots, 13$. The constraints (10), $(B2)$–$(B4)$, $(B8)$–$(B10)$, $(B17)$–$(B19)$ and $(B21)$–$(B23)$ supply the information

$$\begin{gathered} q_{8i} = 1, \quad q_{6i} = 0, \quad i = 1, \ldots, 8; \\ q_{8i} = 4, \quad q_{6i} \geq 3, \quad q_{4i} \geq 2, \\ q_{2i} = 0, \quad i = 9, \ldots, 13; \\ \deg P_6 + \sum_{i=1}^{13} q_{6i} \leq 21, \quad \deg P_4 + \sum_{i=1}^{13} q_{4i} \leq 14, \\ \deg P_2 + \sum_{i=1}^{13} q_{2i} = 8. \end{gathered} \tag{26}$$

The necessary condition (17) for the edges of the underlying Schwarz triangles to be the images of plane lines of curvature and/or linear asymptotes further implies

$$\deg P_6 + \sum_{i=1}^{14} q_{6i} = 24, \quad \deg P_4 + \sum_{i=1}^{14} q_{4i} = 16, \tag{27}$$

where we define the order at infinity $q_{M,14} = q_{Mi}$, $i = 9, \ldots, 13$. Hence, from (9) and $(C8)$, we have

$$\begin{aligned} a_8(\omega) &= \alpha_8 p_1^4 p_2, \quad a_0(\omega) = \alpha_0, \\ a_6(\omega) &= \alpha_6 P_6(\omega) p_1^{q_{6,9}}, \\ a_4(\omega) &= \alpha_4 P_4(\omega) p_1^{q_{4,9}} p_2^{q_{4,1}}, \\ a_2(\omega) &= \alpha_2 P_2(\omega) p_2^{q_{2,1}}, \end{aligned} \tag{28}$$

subject to the constraints

$$\begin{aligned} \deg P_6 + 6q_{6,9} = 24: &\quad q_{6,9} \geq 3; \\ \deg P_4 + 8q_{4,1} + 6q_{4,9} = 16: &\quad q_{4,9} \geq 2; \\ \deg P_2 + 8q_{2,1} = 8. & \end{aligned} \tag{29}$$

Also, as each $P_M(\omega)$ is a symmetric polynomial with respect to the Schwarz case 4 tiling, if $P_M(\omega)$ is non-constant, then, with $P_M(\omega_i) \neq 0$ by definition, $\deg P_M$ must be some multiple of 12. Equations (29) then imply that $P_6 \equiv 1$, $q_{6,9} = 4$ and $P_2 \equiv 1$, $q_{2,1} = 1$, while the equation for $a_4(\omega)$ has no integral solutions consistent with the constraints and hence this term cannot be present, *i.e.* $\alpha_4 = 0$. In summary, the polynomial equation (1) for the C(P)-surface Weierstrass function has the form

$$\alpha_8 p_1^4 p_2 R^8 + \alpha_6 p_1^4 R^6 + \alpha_2 p_2 R^2 + \alpha_0 = 0. \tag{30}$$

From (14), the constant coefficients α_M are real since a segment of the real axis is a plane-line-of-curvature image. Accordingly, two of these values are arbitrary *via* the homogeneity of (30) and the choice of scaling of the Weierstrass function, *i.e.* the Cartesian coordinate units. Considerations of the polynomial discriminant, as discussed in § 5, yield two homogeneous relations in the coefficients, thus specifying the C(P) surface completely.

In particular, consider the Riemann-surface structure above any one of the twelve $\pi/2$ vertices of the underlying tiling. On the four pairs of identically tessellated sheets, the coverings of this vertex correspond to the four possible positions of the polygon pair with common edge containing the point. These four positions are of two distinct types, generated by the two $\pi/2$ vertices of the underlying tiling residing on the boundary in Fig. 1. Each of these two types gives two coverings, related by reflection in the underlying tile edge intersecting the polygon edge at the $\pi/2$ vertex under consideration. Hence, under the pair of reflection operations yielding the four polygons constituting the two coverings of this type, the $\pi/2$ vertex is the only fixed point and the coverings are locally indistinguishable there. Consequently, the Weierstrass-function values on these two sheets

(unbranched) above this vertex are equal. The discriminant of (30) is thus zero at the twelve $\pi/2$ vertex images of the underlying tiling; more specifically, this equation must yield a pair of repeated roots of R^2 there.

On substitution of the $\pi/2$ vertex positions $\omega = \exp(i\pi/4)\exp(im\pi/2)$ $(m \in \mathbb{Z})$ into $(C8)$ and (30), this implies that there exist numbers a, b and c such that

$$192\alpha_8 R^8 - 16\alpha_6 R^6 - 12\alpha_2 R^2 + \alpha_0 = (aR^4 + bR^2 + c)^2$$

and thus, for consistency, that

$$\alpha_2\alpha_6 = -8\alpha_0\alpha_8, \quad \alpha_0\alpha_6^2 = 108\alpha_8\alpha_2^2. \qquad (31)$$

These are the pair of homogeneous relations completing the parametrization of the C(P) surface. One may trivially check that, on substitution of the coefficient polynomials of (30) into the quartic discriminant formula (25), the relations (31) imply *via* $(C2)$ that

$$D = -27\alpha_2^4\alpha_8^3 p_1^4 p_2^9 p_3^4.$$

Thus, with the degenerate prefactors ignored, the $\pi/2$ vertex images are the only non-trivial zeros of the discriminant.

One of the class of solutions of (31), which are all equivalent up to scaling, is $\alpha_8 = \frac{1}{3}$, $\alpha_6 = -4$, $\alpha_2 = \frac{2}{3}$, $\alpha_0 = 1$. Accordingly, the Weierstrass function of the C(P) surface is the solution set $R = R(\omega)$ of

$$\tfrac{1}{3}p_1^4 p_2 R^8 - 4p_1^4 R^6 + \tfrac{2}{3}p_2 R^2 + 1 = 0 \qquad (32)$$

[where p_1 and p_2 are given in $(C8)$], which recovers the result of Neovius (1883). The explicit solution of (32) may be obtained *via* the standard quartic root formula and simplified using the compact discriminant expression above.

(*b*) *The H′-T surface*

Having illustrated the validity and practicality of the method, we employ it to parametrize the H′-T surface proposed by Schoen and modelled in Fig. 13 of his report (Schoen, 1970). The Gauss-map image of the H′-T *Flächenstück* (bounded entirely by mirror planes) is given here, with reference to the Schwarz case 1 $n = 6$ tiling, in Fig. 2. This polygon, comprising three underlying Schwarz triangles, contains only a single first-order branch point, lying on a triangle edge, so that the set $\{\{b'_{pk}\}_{p=1}^{3}\}_{k=1}^{1} = \{1, 1, 0\}$ is a solution of (24). Repeated reflection in the bounding edges generates 24 distinct polygon positions tessellating a triple covering of the unit sphere and hence the three-sheeted Riemann surface, since the H′-T surface genus $g = 4$ (Schoen, 1970) implies $s = 3$. Analysis of the branched structure of the Riemann surface reveals that the underlying triangle edges lying along the alternate rays $\arg\omega = (2m+1)\pi/6$ are each covered twice by a pair of polygons related by reflection in the edge, on which the boundary wraps around the branch point pinning the two sheets there, and once by the two polygons sharing an unbranched boundary segment coinciding with this edge.

The set of 12 flat-point normal-vector images comprises $\{\omega_i\}_{i=1}^{12} = \{\{A, 1/A\}\exp[i(2m+1)\pi/6]\}$, where $0 < A < 1$, with the corresponding sets $\{N_{ij}, b_{ij}\}_{j=0}^{1}$ given by $\{\{1, 0\}, \{1, 1\}\}$ for each $i = 1, \ldots, 12$. The constraints (10), $(B2)$–$(B4)$, $(B8)$–$(B10)$ and $(B13)$–$(B14)$ of asymptotics demand that $\deg P_M$ and q_{Mi} (identical for each $i = 1, \ldots, 12$) satisfy

$$q_{3i} = 1, \quad q_{2i} \geq 1, \quad q_{1i} = 0, \quad i = 1, \ldots, 12,$$

$$\deg P_2 + \sum_{i=1}^{12} q_{2i} \leq 8, \quad \deg P_1 \leq 4,$$

and the necessary condition (17) implies that these last two constraints are strict equalities. The two conditions for $M = 2$ cannot be reconciled so $\alpha_2 = 0$. The symmetry of the underlying tiling then implies that the H′-T polynomial equation (1) has the form

$$\alpha_3(p_2^2 - \gamma_3 p_1^6)R^3 + \alpha_1 p_1^2 R + \alpha_0 = 0, \qquad (33)$$

where p_1 and p_2 are given by $(C9)$ (for $n = 6$) and, from equations $(C4)$–$(C5)$, $\prod_{i=1}^{12}(\omega - \omega_i) = p_2^2 - \gamma_3 p_1^6$, $\gamma_3 < 0$. Since a segment of the real axis is the image of a plane line of curvature, (14) implies that α_3, α_1, α_0 are real.

By virtue of its hexagonal symmetry, the H′-T surface possesses a single degree of freedom, manifested in the normal vector of the flat point on the *Flächenstück*. The one-parameter IPMS family defined by this variable γ_3 is given by (33) in conjunction with an additional homogeneous relation coupling the coefficients α_M (in terms of γ_3). This relation is again furnished by analysis of the polynomial discriminant.

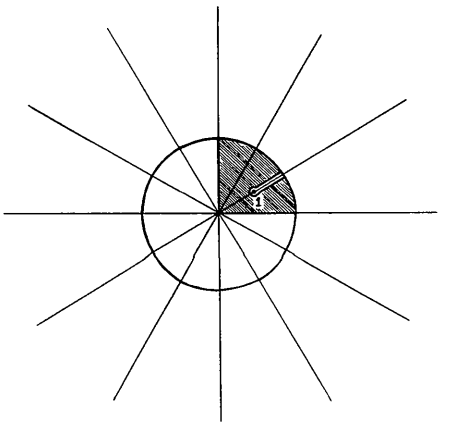

Fig. 2. Projection of the Schwarz case 1 $n = 6$ tiling, the shaded subunit of which represents the Gauss-map image of the H′-T surface *Flächenstück*. The *Flächenstück* boundary consists of five plane lines of curvature (one containing a first-order flat point) meeting orthogonally, so all edges of the image are '*p*'-type segments.

Consider the nature of the polygonal tessellation of the Riemann surface above the set of six $\pi/2$ vertices $\omega = \exp(im\pi/3)$ of the Schwarz tiling. Each such point is covered once by the junction of four polygons with $\pi/2$ vertices situated there and twice by pairs of polygons sharing the common unit-circle edge. The latter two coverings, related by reflection in the ray $\arg \omega = m\pi/3$, thus represent a degeneracy and bear identical Weierstrass-function values there. Equivalently, the discriminant of the polynomial equation (33) vanishes at these special points. Evaluation of the cubic discriminant formula in (25) then implies

$$4\alpha_1^3 + 27(4-\gamma_3)\alpha_0^2\alpha_3 = 0, \qquad (34)$$

which supplies the required homogeneous relation. With (33) and (34) combined, the Weierstrass function of the H′-T surface is thus given by

$$(4-\gamma_3)^{-1}(p_2^2 - \gamma_3 p_1^6)R^3 - 3p_1^2 R \pm 2 = 0: \quad \gamma_3 < 0 \qquad (35)$$

[p_1 and p_2 are those in ($C9$) for $n=6$]. Here, $\pm$ represents the right- and left-handed members of the enantiomorphic pair of H′-T surfaces. The explicit expression for the triple-valued function $R(\omega)$ is readily obtained from (35) by use of the depressed cubic root formula.

(*c*) *The PT surface*

This surface of Koch & Fischer (1989) was discovered empirically by attaching two spouts to each catenoid-like surface patch comprising the oPb surface [as illustrated in Fig. 12 of Fischer & Koch (1990)]. Since the PT genus $g=5$, the Riemann surface is four-sheeted, constructed from two identical copies of the double covering tessellated by the Gauss-map image of the *Flächenstück*, given with respect to the Schwarz case 1 $n=2$ tiling in Fig. 3.

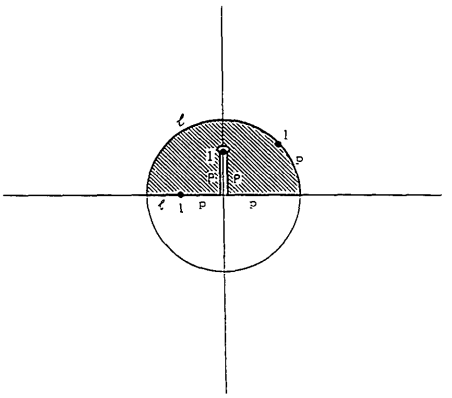

Fig. 3. The projected Gauss-map image of the PT surface *Flächenstück*, displayed with respect to the Schwarz case 1 $n=2$ tiling. The boundary is constructed from six perpendicularly intersecting segments - four plane lines of curvature 'p' and a pair of linear asymptotes 'l'.

Again, the two identical copies, resulting from the presence of on-surface inversion centres (at the first-order branch points where plane line of curvature and linear asymptotes intersect perpendicularly), bear equal and opposite Weierstrass-function values $R(\omega)$ for each ω, implying that the quartic polynomial equation (1) is now quadratic in R^2. The underlying triangle edges along the real axis and the unit circle coincide with an identical pair of polygon edges pinned at a first-order branch point on two sheets and with a second identical pair of unbranched polygon edges on the remaining two sheets. The segments along the imaginary axis coincide with two pairs of identical polygons with boundaries wrapping around the branch point (pinning a sheet of each pair) and the two coverings related by imaginary-axis reflection.

The set of 12 flat-point normal-vector images comprise $\{\omega_i\}_{i=1}^4 = \{\exp[i(m\pi \pm \theta)]\}$, where $0 < \theta < \pi/2$,

$$\{\omega_i\}_{i=5}^8 = \{\{A, 1/A\}\exp(im\pi)\}$$

and

$$\{\omega_i\}_{i=9}^{12} = \{\{B, 1/B\}\exp[i(2m+1)\pi/2]\},$$

where $0 < A, B < 1$. The constraints on the coefficient polynomials $a_M(\omega)$, $M = 4, 2, 0$, are now

$$q_{4i} = 1, \quad q_{2i} = 0, \quad i = 1, \ldots, 8,$$
$$q_{4i} = 2, \quad q_{2i} \geq 1, \quad i = 9, \ldots, 12,$$
$$\deg P_2 + 4q_{2,9} = 8.$$

This implies that the form of the PT polynomial equation (1) is

$$\alpha_4(p_2^2 - \gamma_1 p_1^2)(p_2^2 - \gamma_2 p_1^2)(p_2^2 - \gamma_3 p_1^2)^2 R^4 + \alpha_2(p_2^2 - \gamma_0 p_1^2)(p_2^2 - \gamma_3 p_1^2)R^2 + \alpha_0 = 0, \qquad (36)$$

where p_1 and p_2 are again defined by ($C9$) (for $n=2$), γ_0 is some real number and the parameters γ_1, γ_2, γ_3 are the degrees of freedom in the symmetric forms representing the branch-point polynomials of the three edge types in Fig. 3:

$$\prod_{i=1}^{4}(\omega - \omega_i) = p_2^2 - \gamma_1 p_1^2, \quad 0 < \gamma_1 < 4;$$

$$\prod_{i=5}^{8}(\omega - \omega_i) = p_2^2 - \gamma_2 p_1^2, \quad \gamma_2 > 4;$$

and

$$\prod_{i=9}^{12}(\omega - \omega_i) = p_2^2 - \gamma_3 p_1^2, \quad \gamma_3 < 0.$$

Furthermore, the coefficients α_4, α_2 and α_0 are all real since a segment of the real axis is a plane-line-of-curvature image.

As the PT surface is orthorhombic, it is defined (up to a uniform dilation) by a two-parameter family. Now (36) contains the real parameters α_4, α_2, α_0

(two of which are arbitrary) and γ_0, γ_1, γ_2, γ_3. Thus the PT family corresponds to a subclass of this general equation obtained *via* the imposition of three additional constraints.

From consideration of Fig. 3, at the branch points $\{\omega_i\}_{i=9}^{12}$ and the points $\pm i$, the shaded polygon unit subtends angles (of 2π and π, respectively) double that of the underlying Schwarz tiling. Consequently, the two pairs of function values on the Riemann surface above these sites must coincide, that is, the discriminant of the polynomial equation (36) must vanish for $p_2^2-\gamma_3 p_1^2=0$ and $p_2^2=0$. Substitution into the familiar quadratic discriminant formula (25) then supplies the two relations

$$\gamma_0^2\alpha_2^2-4\gamma_1\gamma_2\alpha_0\alpha_4=0, \tag{37}$$

$$\gamma_0(\gamma_0-\gamma_1)(\gamma_0-\gamma_2)-(\gamma_0^2-\gamma_1\gamma_2)(\gamma_0-\gamma_3)=0. \tag{38}$$

Owing to this quadratic nature, (36) may then be simply solved to give

$$\begin{aligned} R=\pm\{&[-(p_2^2-\gamma_0 p_1^2)\pm(1-\gamma_0^2/\gamma_1\gamma_2)^{1/2}\\ &\times p_2(p_2^2-\gamma_3 p_1^2)^{1/2}][(p_2^2-\gamma_1 p_1^2)\\ &\times(p_2^2-\gamma_2 p_1^2)(p_2^2-\gamma_3 p_1^2)]^{-1}\}^{1/2}, \end{aligned} \tag{39}$$

subject to the supplementary relation (38).

As such, the Weierstrass function contains the three branch-point variables γ_1, γ_2, γ_3 and thus generates a three-parameter surface family. In this example, discriminant conditions alone are insufficient to specify completely the true IPMS family. The reason is apparent from the form of the IPMS fundamental unit (Fischer & Koch, 1990). The three-parameter description refers to the generic noncrystallographic case in which the length of the protruding spout-like attachment is arbitrary. The two-parameter PT surface is the special case for which the spout length is half that of the corresponding edges of the rectangles spanned by the catenoid. This additional constraint is formulated *via* substitution of the Weierstrass function into the representation (11) and relating the pair of path integrals defining the two lengths (the details of which are not given here). This example illustrates the more complicated parametrizations necessitating introduction of additional global constraints to which the Gauss map is insensitive - specifically, the requirement that continuation of the fundamental surface unit gives rise to a crystallographic IPMS.

(*d*) *The pCLP and VAL surfaces*

The list of regular-class solutions in paper II contained a new (non-crystallographic) pentagonal surface and a new orthorhombic (non-self-intersecting) IPMS, denoted pCLP and VAL, respectively, the *Flächenstück* of which are illustrated in Figs. 6(*b*) and 17(*b*) of paper II. In both cases, these 'regular' surfaces (which are precisely self-adjoint) are special members of a generic 'irregular' surface family. For the former case, the restriction of regularity demands that the surface-normal vector at the first-order flat point subtends an angle of $\pi/5$ to both edges of the bounding pentagonal prism base meeting there. Consequently, the ratio of the prism dimensions is restricted to a particular value. Variation of this flat-point normal vector then produces the generic one-parameter pCLP surface family, corresponding to an arbitrary stretching of the bounding prism in the vertical direction. In the VAL case, the first-order flat-point normal vectors of the 'regular' surface are constrained to be vertical and, accordingly, only two of the three orthorhombic bounding unit dimensions are independently specifiable. Removal of this constraint then produces the general two-parameter VAL IPMS family.

The Gauss-map images of these 'irregular' *Flächenstücke* are represented in Figs. 4 and 5, again with reference to the Schwarz case 1 $n=5$ and $n=2$ underlying tilings of their 'regular' counterparts in Figs. 6(*a*) and 17(*a*) of paper II, respectively. Note that all topological and symmetry properties of the 'regular' surfaces are retained in this (merely mathematical) generalization. Again, this pair of genus 5 surfaces possess on-surface inversion centres, so the defining polynomial equations are quadratic in R^2. The derivations of the forms of these two equations are straightforward and hence are omitted here. The single supplementary homogeneous relation in the (real) constant coefficients is provided by the discriminant, which is zero at the underlying tiling vertices $\omega=\exp[i(2m+1)\pi/5]$ and $\omega=0,\infty$, respectively, in two cases.

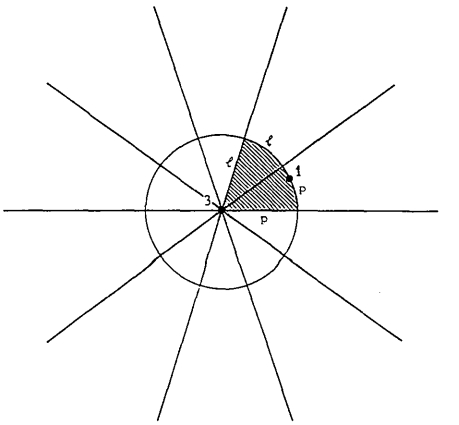

Fig. 4. Gauss-map image of the pCLP *Flächenstück* projected with respect to the Schwarz case 1 $n=5$ tiling. The boundary consists of a pair of perpendicularly intersecting plane lines of curvature 'p' and linear asymptotes 'l', meeting orthogonally at a first-order flat point and subtending an angle of $\pi/10$ at a third-order flat point.

The polynomial equation for the generic pCLP surface is found to be

$$\omega^3[(\omega^5+1)^2-4\cos^2(5\theta/2)\omega^5]R^4 \pm 4\cos(5\theta/2)\omega^4R^2-1=0, \quad (40)$$

where $0<\theta\leq\pi/5$ is the argument of the first-order flat-point normal-vector image in Fig. 4. The equation for the generic VAL IPMS is

$$[(\omega^2+1)^2-4\cos^2(\theta)\omega^2]^3\{(\omega^2+1)^2 -2[1+\tfrac{1}{2}(A^2+1/A^2)]\omega^2\}R^4 \pm 2[(\omega^2+1)^2-4\cos^2(\theta)\omega^2]^2R^2+1=0, \quad (41)$$

where now $0<\theta<\pi/2$ is the argument of the third-order branch point and $0<A<1$ is the value of the first-order branch point inside the unit circle shown in Fig. 5. In both cases, $\pm$ denotes, respectively, the surface or the adjoint surface, which together define a continuous self-adjoint family. The one exactly self-adjoint member of this family is the regular-class surface (given in rows 6 and 17 of Table II1), corresponding to the value $\theta=\pi/5$ for the pCLP surface and the singular limit $A\to 0$ of the VAL surface, as expected.

The author thanks Dr S. T. Hyde and Dr S. Lidin for their helpful criticisms.

APPENDIX *A*

Compactness of the IPMS fundamental unit implies that any singularity of $R(\omega)$ at $\omega=\omega_i$ is integrable and hence $a_{ij}\leq b_{ij}$. If the surface is reoriented such that the normal vector of the flat point of interest coincides with the negative z axis and thus with $\omega_i=0$, the surface is invariant on clockwise rotation of an angle φ' about the z axis provided the representation (I1) possesses the property (II11), which implies that the branches of the Weierstrass function pinned at the branch point b_{ij} satisfy the functional relation (II12). This is the case only if the asymptotic form (7) satisfies this equation locally, which yields the necessary condition on the rotation angle φ' of

$$\exp\{i\varphi'[2-a_{ij}/(b_{ij}+1)]\}=1. \quad (A1)$$

Recall that, in the Gauss map, the angle of intersection of any two geodesics on the surface at the flat point is increased by the factor $b_{ij}+1$ and the sense of rotation is reversed. Thus, the angle φ', common to the surface and its Gauss-map image in (II11), must satisfy $\varphi'/(b_{ij}+1)=-\varphi' \bmod 2\pi$ or, equivalently,

$$\exp[i\varphi'(b_{ij}+2)/(b_{ij}+1)]=1. \quad (A2)$$

On elimination of φ' from the above pair of equations, the inequality $a_{ij}\leq b_{ij}$ then implies

$$a_{ij}=b_{ij}. \quad (A3)$$

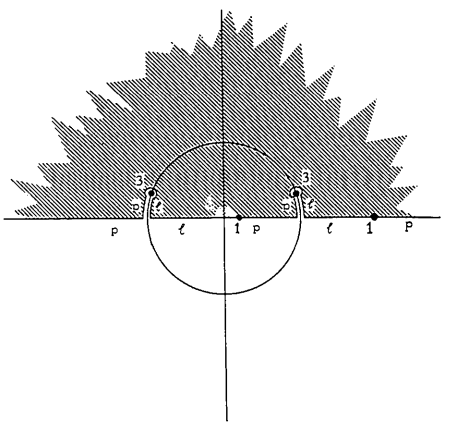

Fig. 5. Image of the VAL *Flächenstück* projected with respect to the Schwarz case 1 $n=2$ tiling. The *Flächenstück* is delimited by two pairs of perpendicularly intersecting plane lines of curvature 'p' and linear asymptotes 'l', alternately joined (orthogonally) at first- and third-order flat points.

APPENDIX *B*

Combination of (8) and (9) gives

$$a_M(\omega)R^M \sim \alpha_M P_M(\omega_i)\beta_{Mi}\gamma_{ij}^M \times(\omega-\omega_i)^{q_{Mi}-Mb_{ij}/(b_{ij}+1)}, \quad \omega\to\omega_i:$$

$$\beta_{Mi}=\prod_{\substack{k=1\\k\neq i}}^{n}(\omega_i-\omega_k)^{q_{Mk}}. \quad (B1)$$

Recall that the $b_{ij}+1$ branches of the Weierstrass function pinned at a branch point of order b_{ij} above ω_i correspond locally to the values of γ_{ij} given by the $b_{ij}+1$ roots of a complex number r_{ij} [in (7)]. As there are N_{ij} such branch points over ω_i, substitution of (*B*1) into (1) must yield, to leading order in $\omega-\omega_i$, a polynomial of degree N_{ij} in $\gamma_{ij}^{b_{ij}+1}$. The sth term in (1) defines the Riemann-surface branch points and, in combination with remaining terms, specifies the nature of the branch-point structure. Hence, we require that, to leading asymptotic order, the $M=s$ and $M=s-N_{ij}(b_{ij}+1)$ terms in (1) are of equal order, with the $N_{ij}-1$ intermediate terms in the equivalence class modulo $b_{ij}+1$ given by $M=s-m(b_{ij}+1)$, $m=1,\ldots,N_{ij}-1$, of order no lower than this, and the remaining $s-N_{ij}$ terms of strictly higher order. This determines the value of $q_{s-N_{ij}(b_{ij}+1),i}$ in terms of the quantity q_{si} defined in (10),

$$q_{s-N_{ij}(b_{ij}+1),i}+N_{ij}b_{ij}=q_{si}, \quad (B2)$$

and imposes the inequalities

$$q_{s-m(b_{ij}+1),i}+mb_{ij}\geq q_{si}, \quad m=1,\ldots,N_{ij}-1 \quad (B3)$$

on the intermediate q_{Mi} values and the strict inequalities

$$q_{Mi}+(s-M)b_{ij}/(b_{ij}+1)>q_{si} \qquad (B4)$$

on the remaining $s-N_{ij}$ values of q_{Mi}. The N_{ij} values of $\gamma_{ij}^{(b_{ij}+1)}$ (which are strictly non-zero) are then given, on combination of (1) and (B1), by the polynomial equation

$$\sum_{m=0}^{N_{ij}}{}' \alpha_{s-m(b_{ij}+1)}P_{s-m(b_{ij}+1)}(\omega_i)\beta_{s-m(b_{ij}+1),i} \times(\gamma_{ij}^{-(b_{ij}+1)})^m=0, \qquad (B5)$$

where the prime on the summation indicates the inclusion of only those intermediate terms for which the condition (B3) is a strict equality. (This convention will be used throughout Appendix B).

In the special case $j=0$, the branch-point order is zero and, on substitution of $b_{i0}=0$ into (8), the asymptotic form reduces to

$$R(\omega)\sim\gamma_{i0}, \quad \omega\to\omega_i \qquad (B6)$$

on an unbranched sheet above ω_i. By analogy with (B1), we have

$$a_M(\omega)R^M\sim\alpha_M P_M(\omega_i)\beta_{Mi}\gamma_{i0}^M \times(\omega-\omega_i)^{q_{Mi}}, \quad \omega\to\omega_i, \qquad (B7)$$

which, when combined with (1), must produce, to leading (namely zeroth) order in $\omega-\omega_i$, a polynomial of degree N_{i0} for the function values γ_{i0} on the N_{i0} such unbranched sheets. Thus, since the zeroth term in the polynomial equation (1) is constant, we require that the term $M=N_{i0}$ in (1) is likewise of order zero, with the intermediate terms $M=1,\ldots,N_{i0}-1$ of non-negative order and the remaining terms of strictly positive order,

$$q_{N_{i0},i}=q_{0i}=0, \qquad (B8)$$

$$q_{Mi}\geq 0, \quad M=1,\ldots,N_{i0}-1, \qquad (B9)$$

$$q_{Mi}>0, \quad M=N_{i0}+1,\ldots,s. \qquad (B10)$$

Then, as above, the N_{i0} values of γ_{i0} are specified by the polynomial equation

$$\sum_{M=0}^{N_{i0}}{}' \alpha_M P_M(\omega_i)\beta_{Mi}\gamma_{i0}^M=0. \qquad (B11)$$

With the assumption, without loss of generality, that each flat-point normal-vector image ω_i is finite and with the corresponding sequence $\{q_{Mi}\}_{M=0}^{s}$ thus constrained by the above conditions, the point at infinity in the closed complex plane is not a flat-point image. Thus, the s sheets of the Riemann surface over ∞ are unbranched and, from (I2), the Weierstrass function has the asymptotic form (I5),

$$R(\omega)\sim\gamma_\infty\omega^{-4}, \quad \omega\to\infty. \qquad (B12)$$

The implications of the requirement that the polynomial equation (1) yields s values of γ_∞ in the limit $\omega\to\infty$ are discussed in the Appendix of paper I. In particular, this imposes the constraints

$$\sum_{i=1}^{n} q_{si}=4s, \qquad (B13)$$

$$\deg P_M+\sum_{i=1}^{n} q_{Mi}\leq 4M, \quad M=1,\ldots,s-1 \qquad (B14)$$

(where $\deg P_M$ is the degree of P_M) and supplies the polynomial equation

$$\sum_{M=0}^{s}{}' \alpha_M\gamma_\infty^M=0 \qquad (B15)$$

for the s values of γ_∞. Equation (B13) is satisfied identically by virtue of (6) and (10), leaving the non-trivial constraint (B14) relating the sequence $\{q_{Mi}\}_{i=1}^{n}$ to $\deg P_M$.

For IPMS of certain symmetries, it is convenient to choose a coordinate orientation such that a flat point is mapped to the point at infinity in the closed complex plane. If $\omega_n=\infty$ then (8)–(10) and (B1)–(B11) still apply to the set of finite branch points $\{\omega_i\}_{i=1}^{n-1}$ [with the product range in (9) and (B1) now restricted to $1\leq i\leq n-1$], while the conditions (B12)–(B15) are replaced by the following constraints. If the asymptotic form

$$R(\omega)\sim\gamma_{nj}\omega^{-4+b_{nj}/(b_{nj}+1)}, \quad \omega\to\infty \qquad (B16)$$

is inserted into (1), consistency with the branch-point structure under ω_n demands that, for $j=1,\ldots,n_n$,

$$\deg P_{s-N_{nj}(b_{nj}+1)}+\sum_{i=1}^{n-1} q_{s-N_{nj}(b_{nj}+1),i} +4N_{nj}(b_{nj}+1)-N_{nj}b_{nj}=\sum_{i=1}^{n-1} q_{si}, \qquad (B17)$$

$$\deg P_{s-m(b_{nj}+1)}+\sum_{i=1}^{n-1} q_{s-m(b_{nj}+1),i}+4m(b_{nj}+1)-mb_{nj} \leq\sum_{i=1}^{n-1} q_{si}, \quad m=1,\ldots,N_{nj}-1, \qquad (B18)$$

and

$$\deg P_M+\sum_{i=1}^{n-1} q_{Mi}+4(s-M) -(s-M)\,b_{nj}/(b_{nj}+1)<\sum_{i=1}^{n-1} q_{si}, \qquad (B19)$$

where the last condition applies to the remaining $s-N_{nj}$ values of M. Accordingly, the N_{nj} values of $\gamma_{nj}^{b_{nj}+1}$ are specified by the polynomial equation

$$\sum_{m=0}^{N_{nj}}{}' \alpha_{s-m(b_{nj}+1)}(\gamma_{nj}^{-(b_{nj}+1)})^m=0. \qquad (B20)$$

On the N_{n0} unbranched sheets under ω_n, the Weierstrass-function asymptotic form, given by substituting $j=0$ and $b_{nj}=b_{n0}=0$ into (*B*16), yields the constraints

$$\deg P_{N_{n0}}+\sum_{i=1}^{n-1} q_{N_{n0},i}=4N_{n0}, \qquad (B21)$$

$$\deg P_M+\sum_{i=1}^{n-1} q_{Mi}\leq 4M, \quad M=1,\ldots,N_{n0}-1, \qquad (B22)$$

$$\deg P_M+\sum_{i=1}^{n-1} q_{Mi}<4M, \quad M=N_{n0}+1,\ldots,s \qquad (B23)$$

and the polynomial equation

$$\sum_{M=0}^{N_{n0}}{}' \alpha_M \gamma_{n0}^M=0. \qquad (B24)$$

APPENDIX *C*

With the vertices of the Schwarz triangle with angles $\lambda_j\pi$, denoted by ν_j, the opposite edges by e_j and the single face by f, the numbers of each in the tessellation are given by (I34). For convenience, a coordinate orientation is chosen such that, in projection, a vertex ν_1 resides at infinity and an edge e_2 lies along a real-axis segment. The polynomials

$$p_{\nu_j}\equiv p_j=\prod_{\substack{q=1\\ \omega_{jq}\neq\infty}}^{V_j}(\omega-\omega_{jq}), \quad j=1,2,3 \qquad (C1)$$

(with zeros the finite images ω_{jq} of the tessellation vertices of type j and degree V_j counted with the suppressed zero at infinity), are the lowest-degree symmetric polynomials of the tiling. Furthermore, the set of polynomials $\{p_j^{1/\lambda_j}(\omega)\}_{j=1}^3$ is linearly dependent - in particular there exists a real constant γ such that

$$p_3^{1/\lambda_3}=p_2^{1/\lambda_2}-\gamma p_1^{1/\lambda_1}. \qquad (C2)$$

The polynomial forms

$$p_{e_j}=\prod_{q=1}^{E_j}(\omega-\omega_{e_j,q}), \quad j=1,2,3, \qquad (C3)$$

generated by the set of images $\omega_{e_j,q}$ of a general point on the triangle edge e_j, define symmetric polynomial one-parameter families of common degree $E_j=E$. Equivalently, these may be expressed as

$$p_{e_j}=p_2^{1/\lambda_2}-\gamma_j p_1^{1/\lambda_1}, \qquad (C4)$$

where the three edge types e_j correspond to the ranges of the real parameter γ_j

$$\gamma_3<0, \quad 0<\gamma_1<\gamma \quad \text{and} \quad \gamma_2>\gamma \quad \text{if } \gamma>0 \qquad (C5)$$

(with the signs of γ and the γ_j reversed if $\gamma<0$). The maximal-degree basic symmetric form is the two-parameter polynomial family

$$p_f=\prod_{q=1}^{F}(\omega-\omega_{fq}), \qquad (C6)$$

with zeros the tessellation images ω_{fq} of a general point in the triangle interior f. It may likewise be expressed in terms of the vertex polynomials as

$$p_f=(p_2^{1/\lambda_2}-\gamma_f p_1^{1/\lambda_1})(p_2^{1/\lambda_2}-\bar{\gamma}_f p_1^{1/\lambda_1}) \qquad (C7)$$

for some complex parameter γ_f.

In particular, for the Schwarz case 4 tessellation (the underlying tiling shown in projection in Fig. 1), the vertex angles are $(\lambda_1,\lambda_2,\lambda_3)\pi=(\frac{1}{4},\frac{1}{3},\frac{1}{2})\pi$, for which the sets of 6, 8 and 12 tessellation vertex images are

$$\{0,\infty,\exp(im\pi/2)\},$$

$$\{[(3^{1/2}\pm 1)/2^{1/2}]\exp(i\pi/4)\exp(im\pi/2)\}$$

and

$$\{\{2^{1/2}\pm 1,\exp(i\pi/4)\}\exp(im\pi/2)\},$$

respectively (where $m\in\mathbb{Z}$), in the chosen orientation. Hence, from (*C*1), the λ_1 and λ_2 vertex polynomials (in terms of which all other symmetric forms can be expressed) are

$$p_1=\omega(\omega^4-1), \quad p_2=\omega^8+14\omega^4+1, \qquad (C8)$$

and the value of γ in (*C*2) is 108. In the Schwarz case 1 family with vertex angles $(\lambda_1,\lambda_2,\lambda_3)\pi=(\frac{1}{n},\frac{1}{2},\frac{1}{2})\pi$ for $n\geq 2$ (for example, $n=6$ subcase is the underlying tiling projected in Fig. 2), the sets of 2, n and n images of each vertex type are $\{0,\infty\}$, $\{\exp(i\pi/n)\exp(i2m\pi/n)\}$ and $\{\exp(i2m\pi/n)\}$, respectively. The λ_1 and λ_2 vertex polynomials are then

$$p_1=\omega, \quad p_2=\omega^n+1 \qquad (C9)$$

and the corresponding γ value is now 4.

References

ERDÉLYI, A., MAGNUS, W., OBERHETTINGER, F. & TRICOMI, F. G. (1953). *Higher Transcendental Functions.* Bateman Manuscript Project. New York: McGraw-Hill.

FISCHER, W. & KOCH, E. (1987). *Z. Kristallogr.* **179**, 31-52.

FISCHER, W. & KOCH, E. (1989). *Acta Cryst.* A**45**, 726-732.

FISCHER, W. & KOCH, E. (1990). *J. Phys. (Paris) Colloq.* C7, 131-147.

FOGDEN, A. & HYDE, S. T. (1992*a*). *Acta Cryst.* A**48**, 442-451.

FOGDEN, A. & HYDE, S. T. (1992*b*). *Acta Cryst.* A**48**, 575-591.

FONTELL, K. (1990). *Colloid Polym. Sci.* **268**, 264-285.

KOCH, E. & FISCHER, W. (1988). *Z. Kristallogr.* **183**, 129-152.

KOCH, E. & FISCHER, W. (1989). *Acta Cryst.* A**45**, 558-563.

KOCH, E. & FISCHER, W. (1990). *Acta Cryst.* A**46**, 33-40.

LANDH, T. (1992). *J. Phys. Chem.* In the press.

NEOVIUS, E. R. (1883). *Bestimmung Zweier Speciellen Periodische Minimalflächen.* Helsinki: Frenckel.

SCHOEN, A. H. (1970). *Infinite Periodic Minimal Surfaces Without Self-intersections.* NASA Technical Note No. D5541. Washington, DC, USA.